

Experimental investigation of Shedding Mode II in circular cylinder wake

Bc. Lucie Balcarová

Vedoucí práce: Prof. Pavel Šafařík

Abstrakt (Times New Roman, Bold + Italic, 12, řádkování 1)

This work introduces results from experimental investigation of flow behind a circular cylinder. Experiment was performed in a towing tank that is filled with water. The cylinder rotates in counter-clockwise direction with a non-dimensional rotation rate α varying from 0 to 5.6. The measurements were fixed at Reynolds number $Re = 100$. The flow is associated with two-dimensional instabilities. The rotation rate range covers different flow regimes, such as Shedding Mode I, a stable region, Shedding Mode II and then another stable region.. The main objective of this report are to focus on Shedding Mode II and to investigate the corresponding vortical structure. PIV method was used.

Klíčová slova (Times New Roman, Bold + Italic, 12, řádkování 1)

Experiment, rotating cylinder, rotation rate, Reynolds number, Shedding Mode II.

1. Introduction

This project is focused on experimental investigation of flow behind a circular cylinder rotating with a non-dimensional rotation rate α varying from 0 to 5.6 in a towing tank that is filled with water. This rotation rate range covers different flow regimes, such as Shedding Mode I, a stable region, Shedding Mode II and then another stable region. The measurements were performed for Reynolds number $Re = 100$. The main objective of this report are:

- to focus on Shedding Mode II
- to investigate the corresponding vortical structure

The process of the experiment was modified according to the availability of the experimental set-up as well as the time designated for the project.

Particle Image Velocimetry (PIV) technique was used in a towing tank to perform this investigation. PIV analysis of the images was done using PivView and PIVTEC software.

The post-processing of the results was analyzed by Matlab software.

The project was in progress from the end of August 2010 till the end of January 2011.

The previous studies on the subject are described in the literature review. That is followed by the description of experimental set-up and methodologies used during the project. The results are presented towards the end of the report. Discussions with future research proposals about the rotating cylinder are acknowledged in the end of the report.

2. Methodology

2.1 Governing parameters

The flow field is characterized by two parameters, the Reynolds number Re and the rotation rate α :

$$Re = \frac{U_\infty D}{\nu} \quad (1)$$

$$\alpha = \frac{D\omega}{2U_\infty} \quad (2)$$

Here U_∞ is the free-stream velocity, D the cylinder diameter, ν the kinematic viscosity, ω the angular velocity of the rotating cylinder.

The rotation rate in different regions depends on value of the Reynolds number, for example for $Re = 100$ [2]:

- (1) Shedding mode I - $0 \leq \alpha \leq 1.8$
- (2) Stable region - $1.8 < \alpha < 4.8$
- (3) Shedding mode II - $4.8 \leq \alpha \leq 5.1$
- (4) Stable region - $\alpha > 5.1$

The next important dimensionless parameter is the Strouhal number (St):

$$St = \frac{fD}{U_\infty} \quad (3)$$

where f denotes the shedding frequency. The value of Strouhal number depends on the rotation rate.

2.2 Experimental set-up

The experiments were conducted in a towing tank with dimensions $L \times W \times H = 500 \times 50 \times 75 \text{ cm}^3$. The experimental configuration consists of a circular cylinder with a length $L = 480 \text{ mm}$ and diameter $D = 10 \text{ mm}$. The cylinder rotates in the counter-clockwise direction with angular velocity ω , see Figure 1, which is connected by belt to an electric motor. The rotation rate α is changed by setting the voltage of the electric motor. The Reynolds number is fixed to 100. Two cameras are positioned on the side of the tank to record images. Cameras, cylinder and electric motor are fixed to a carriage that moves from right to left with a velocity U_∞ as is shown in Figure 2.

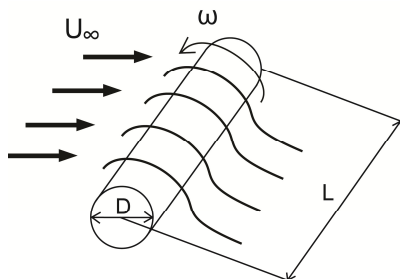


Figure 1 Problem definition

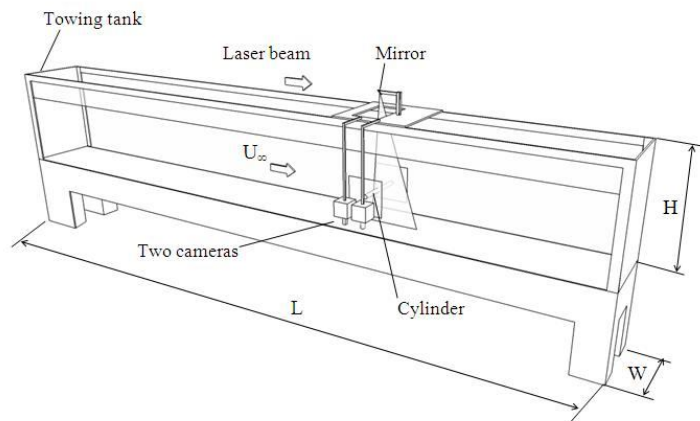


Figure 2 Experimental set-up

2.3 Experimental methods

2.3.1 Particle Image Velocimetry (PIV) method

PIV method was used in experiment. The tank is filled with water which contains small particles. For a good experiment, these particles should have the same density as the fluid and have to be small enough to follow the flow. The particles used in this study have approximately diameter of $d = 20 \mu\text{m}$. They are used in a conjunction with GCR-150 Nd-YAG laser to visualise the flow.

The particles that lay on laser sheet are recorded with two 1.9 megapixel charge-coupled device (CCD) cameras. These are positioned in front of the tank and take images of the flow. By processing the images the displacement of the particles is determined. An image plane is divided into small interrogation areas which are cross-correlated to obtain velocity field.

The principles of PIV are illustrated in Figure 3. Basicly, PIV requires four components:

- (1) An optically transparent test-section containing the flow seeded with tracer particles;
- (2) A light source (laser) to illuminate the region of interest (plane or volume);
- (3) Recording hardware consisting of a CCD camera;
- (4) A computer with suitable software to process the recorded images and extract the velocity information from the tracer. particle positions.

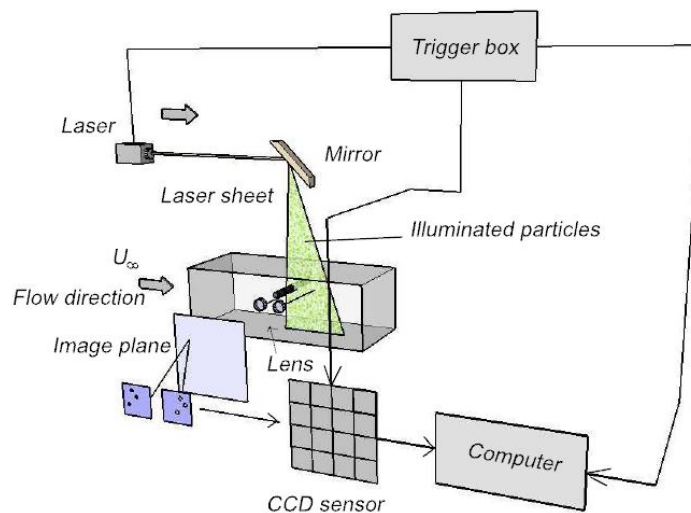


Figure 3 Experimental arrangement for particle image velocimetry

2.3.2 Data processing

The step-by-step process of the data collection and processing is given in Figure 4. The data is obtained using the experimental set-up as described above. Secondly PIV analysis is performed using PivView program [9] where quality of images is analyzed. If the images are with sufficient quality, the final processing is done with the same software and the data files are extracted.

Three types of data are exported for further analysis in Matlab:

- magnitude of displacement velocity,
- vorticity,
- velocity gradient.

Finally, for data visualizations Tecplot software is used.

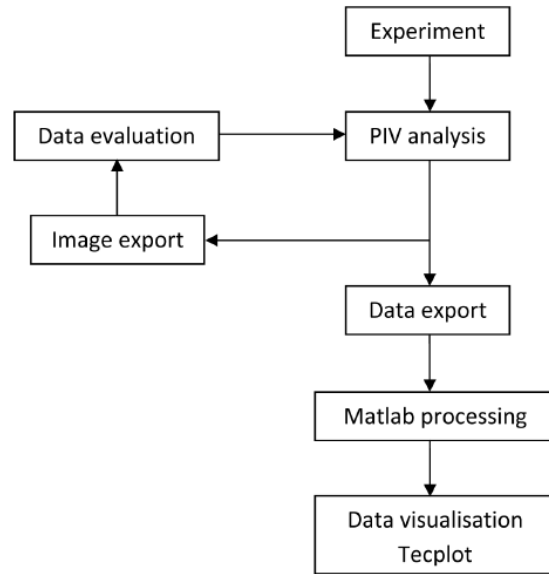


Figure 4 Data processing

2.4 List of measured experiments

List of measured experiments is presented in the Table 1 with corresponding Reynolds number Re , rotation rate α , free stream velocity U_∞ , angular velocity ω , magnification factor M , total frames and region are displayed.

Table 1. – List of measurements

	Re [-]	α [-]	U_∞ [mm/s]	ω [rpm]	M [px/mm]	Num of frames	Remarks
1	100	0	9.809	0	14.55	4000	No rotation
2	100	1.6	10.171	31.10	14.52	4000	Shedding Mode I
3	100	3.0	10.171	58.31	14.52	4300	Stable region
4	100	5.4	10.962	113.11	14.64	4090	Shedding Mode II
5	100	5.45	10.047	104.63	14.64	4390	Shedding Mode II
6	100	5.5	10.047	105.59	14.64	4239	Shedding Mode II
7	100	5.55	10.047	106.55	14.64	4263	Shedding Mode II
8	100	5.6	10.047	107.51	14.64	4279	Stable region

3. Results

3.1 Von Karman Vortex Street ($\alpha = 0$)

Von Karman vortex street is observed for a cylinder with no rotation rate, see Figure 5. This figure shows the data of two frames next to each other. The first frame is from the camera 1 and the second frame is from the camera 2. The data values are averaged at the region where two frames overlap. These frames are placed in non-dimensional coordinates with non-rotation cylinder in origin of axis.

The vortices are generated around the cylinder that moves with a constant free stream velocity $U_\infty = 9.809$ mm/s. The vortex of lower position has a positive vorticity value shown

in blue colour. On the other hand, the upper vortex has a negative vorticity value which is shown in red. The lower vortex grows in size pushing the upper vortex further away from the cylinder. The vortices and their distances are axially symmetrical with respect to $y = 0$. The shedding period T between two lower (or upper) vortices is the same, meaning the flow is fully developed. Then the Strouhal number is calculated as $St = 0.165$. The structure behind cylinder and the Strouhal number confirm the investigation from previous studies [1, 5].

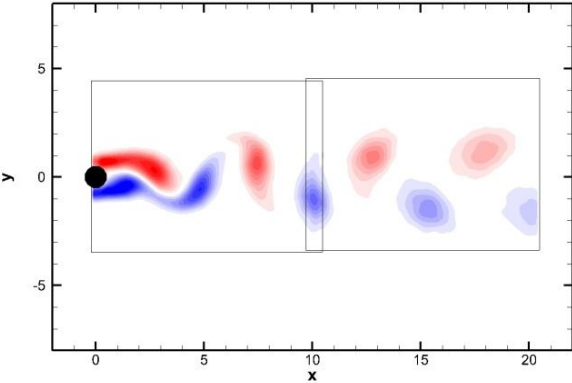


Figure 5 Von Karman vortex street – $\alpha = 0, Re = 100$

3.2 Shedding Mode I ($\alpha = 1.6$)

The flow is unsteady for lower values of α . This regime is called Shedding Mode I, see Figure 6. The rotation rate is relatively slow so a deflected von Karman vortex street can be seen. Two frames are displayed in x - y non-dimensional coordinate system. A rotating cylinder is put into the origin of axis.

The positive and negative vortices grow up with constant velocity $U_\infty = 10.171$ mm/s and rotation rate $\alpha = 1.6$. The trajectory of vortices moves upwards about four degrees with respect to y axis. This displacement is caused by a counter-clockwise direction of a rotating cylinder. The disparity between the flows on the upper and lower surfaces of the cylinder increases with α . The flow is fully developed so the shedding period between the vortices from upper (or lower) surface can be calculated. Consequently, the Strouhal number is computed as $St = 0.164$.

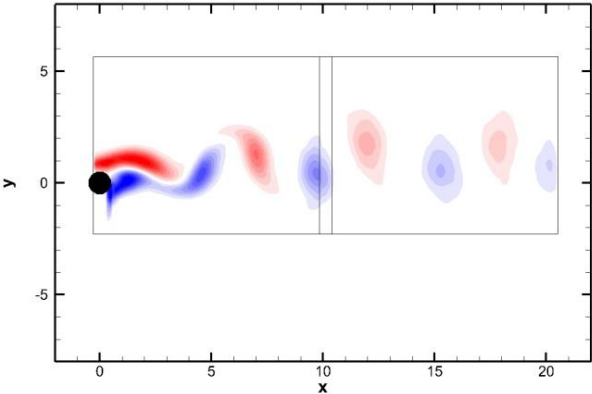


Figure 6 Shedding Mode I – $\alpha = 1.6, Re = 100$

3.3 Stable region ($\alpha = 3.0$)

The vortex shedding of the flow for $1.9 \leq \alpha < 5.4$ achieves a steady state, the evidence can be seen in Figure 7 at $\alpha = 3.0$. Two frames are displayed in x-y non-dimensional coordinate system with the cylinder in the origin of axis. This region is called stable region and is found between the two vortex shedding modes - Shedding Mode I and Shedding Mode II.

The vortex shedding is completely suppressed at this rate of rotation. The shedding period and the Strouhal number can not be calculated without vortices. Therefore, the Strouhal number is $St = 0$.

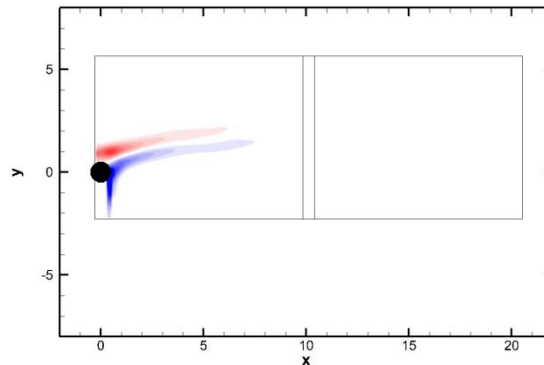


Figure 7 Stable region – $\alpha = 3.0$, $Re = 100$

3.4 Shedding Mode II ($\alpha = 5.40, 5.45, 5.50, 5.55$)

Due to the increased rotation rate, the wake behind the rotating cylinder is not as stable as it was at $\alpha = 3.0$. The flow is in second instability mode for $5.4 \leq \alpha \leq 5.55$. This region is called Shedding Mode II and the instability feature is different from Shedding Mode I. Only vortices from the upper surface of the rotating cylinder are formed. The vortices rotate in the counter-clockwise direction, so does the cylinder. The shedding period between vortices is approximately ten times higher in comparison with von Karman vortices. Therefore, more time for evolution is required to see the phenomenon.

The results for Shedding Mode II are presented in the next sections for different rotation rates. Each section is divided into two subsections:

- (a) vortices,
- (b) shedding process.

The subsection of 'vortices' shows individual vortices or patches that are observed. The subsection of 'shedding process' contains the process of vortex evolution during one period. The amount of vortices and their development is different for each rotation rate. The colours in the images indicate positive (blue) and negative (red) vorticity.

3.4.1 Shedding Mode II ($\alpha = 5.40$)

(a) Vortices – $\alpha = 5.40$

The vorticity around a rotating cylinder at $\alpha = 5.40$ and $U_\infty = 10.962$ mm/s is shown in Figures 8, 9, 10, 11. A clear graphical description of every figure is illustrated in Figure 8. Each figure shows two images. The time between the left and right images is $t = 10$ s. The coordinates are non-dimensional with the rotating cylinder in the origin of axis. Each image

has two frames, one from camera 1 and another from camera 2. The blue colour indicates positive vorticity, the red colour one negative vorticity.

Three separate vortices are identified, Figures 8, 9, 10. They grow from the upper surface of the cylinder and they rotate counter-clockwise. The identified vortices rotate in the same direction, so does the cylinder.

The first vortex develops in a position $y = 8D$ in a distance of approximately $x = 15D$ in the image 2 from camera 2. The second and third vortices appear in the same distance but on a position $y = 6D$.

A slightly rotating vortex can be seen on image 1 in Figure 11. Nevertheless, it does not develop further into a rotating vortex. There is detached vorticity patch on image 2.

The Strouhal number is different amongst individual vortices. A flow is not fully developed. Therefore average Strouhal number from three vortices is calculated as $St = 0.0262$.

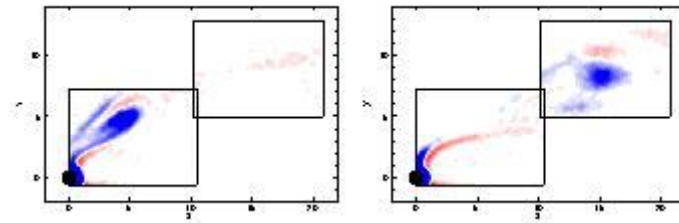


Figure 8 $\alpha = 5.40 - 1. \text{vortex}$

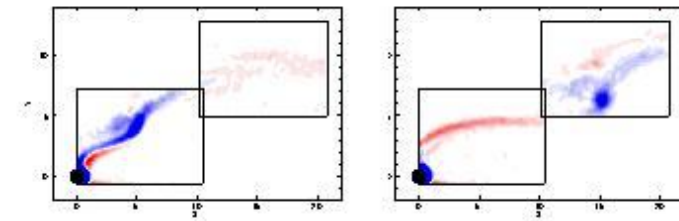


Figure 9 $\alpha = 5.40 - 2. \text{vortex}$

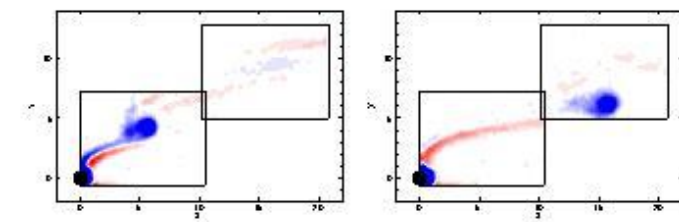


Figure 10 $\alpha = 5.40 - 3. \text{vortex}$

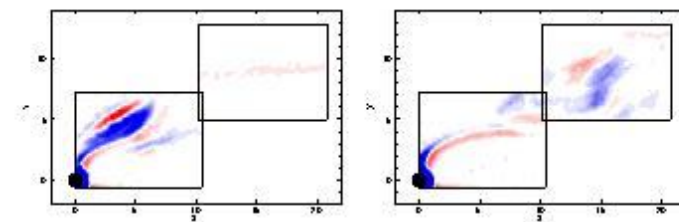


Figure 11 $\alpha = 5.40 - \text{vorticity patch}$

(b) Shedding process – $\alpha = 5.40$

The evolution of the vorticity field over time at $\alpha = 5.4$ is displayed in detail in Figure 12. It also contains the formation and development of the third vortex. The coordinates system is non-dimensional with a rotating cylinder in the origin of axis. The blue colour indicates positive vorticity, the red one negative vorticity. A downstream converting vorticity patch is seen for $t = T/6, 2T/6, 3T/6$.

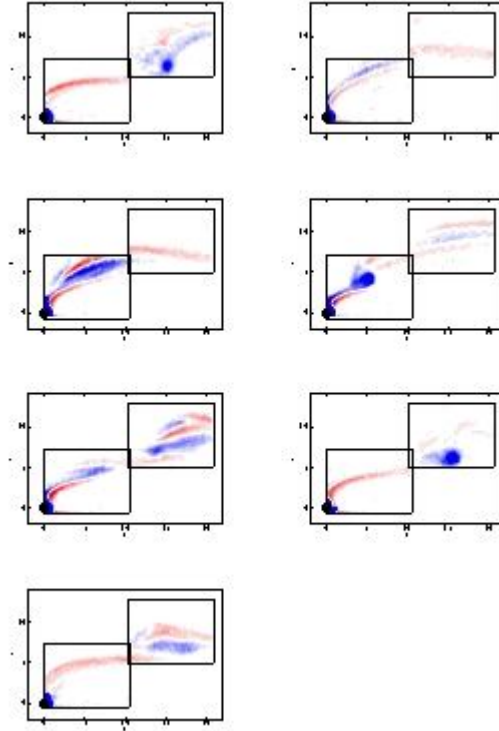


Figure 12 $\alpha = 5.40$ – Shedding process

3.4.2 Shedding Mode II ($\alpha = 5.45$)

(a) Vortices – $\alpha = 5.45$

The vorticity around a rotating cylinder at $\alpha = 5.45$ and $U_\infty = 10.047$ mm/s is shown in Figures 13, 14, 15, 16. A clear graphical description of every figure is illustrated in Figure 8. Each figure shows two images. The time between the left and right images is $t = 10$ s. The coordinates are non-dimensional with the rotating cylinder in the origin of axis. Each image contains two frames, one from camera 1 and another from camera 2. The blue colour indicates positive vorticity, the red one negative vorticity.

Three separate vortices are identified, Figures 13, 15, 16. They grow from the upper surface of the cylinder which rotates counter-clockwise. The identified vortices rotate in the same direction so does the cylinder.

The first vortex already grows in $x = 5D$ in Figure 13 Image 1, but the vortex is not clear anymore in later stages in Image 2. Its position is on $y = 5.5D$.

At the beginning it seems the second vortex starts growing. However, it is developed as a vorticity patch instead, see Figure 14.

The next vortex can be detected easily, see Figure 15. Its shape is very clear and it reaches $y = 6.5D$. The last vortex is in Figure 16 on $y = 6D$ position. The Strouhal number is different amongst individual vortices. The flow is not fully developed so on average Strouhal number from three vortices is calculated as $St = 0.0177$.

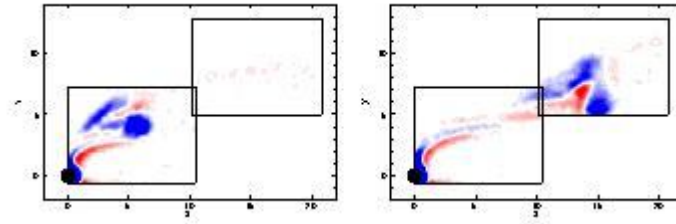


Figure 13 $\alpha = 5.45 - 1.$ vortex

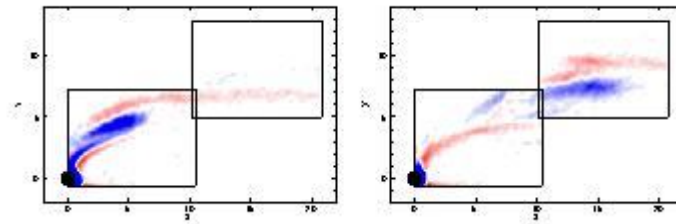


Figure 14 $\alpha = 5.45 -$ vorticity patch

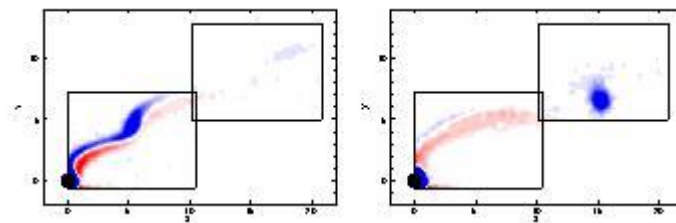


Figure 15 $\alpha = 5.45 - 2.$ vortex

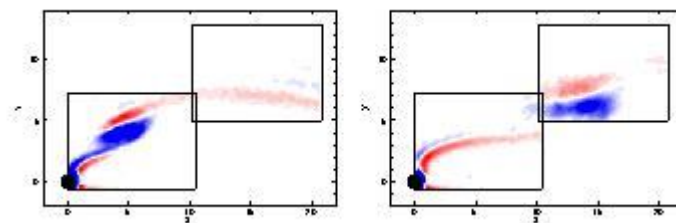


Figure 16 $\alpha = 5.45 - 3.$ vortex

(b) Shedding process – $\alpha = 5.45$

The evolution of the vorticity field over time at $\alpha = 5.45$ is displayed in detail in Figure 17. It also contains the formation and development of the third vortex. The coordinates system is non-dimensional with a rotating cylinder in the origin of axis. The colours in the images indicate positive (blue) and negative (red) vorticity. While the vortex at $t = 0$ is very clear, the shape of the vortex at $t = T$ is wider thus slowly rotation. A downstream converting vorticity patch is seen for $t = 2T/6, 3T/6$.

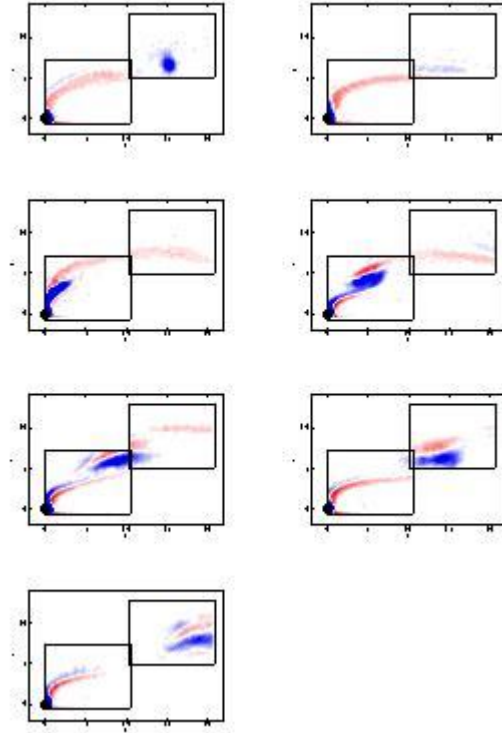


Figure 17 $\alpha = 5.45$ – Shedding process

3.4.3 Shedding Mode II ($\alpha = 5.50$)

The vorticity around a rotating cylinder at $\alpha = 5.50$ and $U_\infty = 10.047$ mm/s is shown in Figures 18, 19. A clear graphical description of every figure is illustrated in Figure 8. Each figure shows two images. The time between the left and right images is $t = 10$ s. The coordinates are non-dimensional with the rotating cylinder in the origin of axis. Each image has two frames, one from camera 1 and another from camera 2. The blue colour indicates positive vorticity, the red one negative vorticity.

The shedding vortices are not detected easily at this rate of rotation. Only vorticity patches are identified at this instant. No vortices are developed therefore the shedding period is zero, so is the Strouhal number.

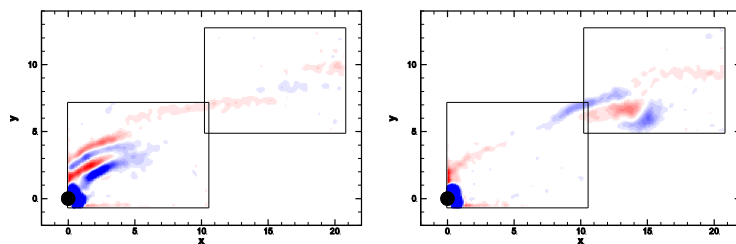


Figure 18 $\alpha = 5.50$ – 1. vorticity patch

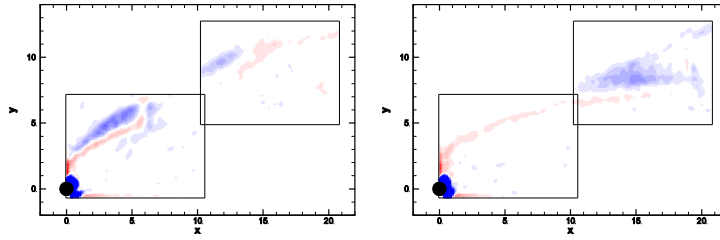


Figure 19 $\alpha = 5.50 - 2$. vorticity patch

3.4.4 Shedding Mode II ($\alpha = 5.55$)

(a) Vortices – $\alpha = 5.55$

The vorticity around a rotating cylinder at $\alpha = 5.55$ and $U_\infty = 10.047$ mm/s is shown in Figures 20, 21, 22, 23. A clear graphical description of every figure is illustrated in Figure 8. Each figure shows two images. The time between the left and the right images is $t = 10$ s. The coordinates are non-dimensional with the rotating cylinder in the origin of axis. Each image contains two frames, one from camera 1 and another from camera 2. The blue colour indicates positive vorticity, the red one negative vorticity.

Three separate vortices are identified, Figures 20, 22, 23. They grow from the upper surface of the cylinder which rotates counter-clockwise. The identified vortices rotate in the same direction, does the cylinder. All vortices have very similar development, shape and position. The vortex grows from the upper surface of the rotating cylinder and drags to the position of about $y = 7D$.

However, the vorticity patch is developed during the flow, see Figure 21. The evolution of vorticity is similar to the vortices, but the rotation of an initial vortex is so small for development one full vortex.

The Strouhal number is different amongst individual vortices. A flow is not fully developed. An average Strouhal number from all vortices is calculated as $St = 0.0123$.

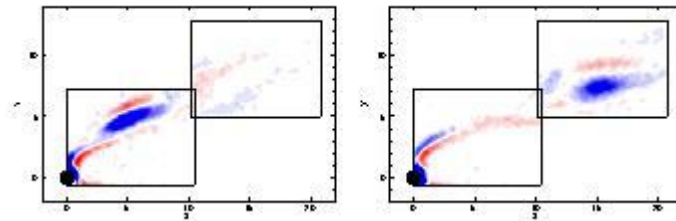


Figure 20 $\alpha = 5.55 - 1$. vortex

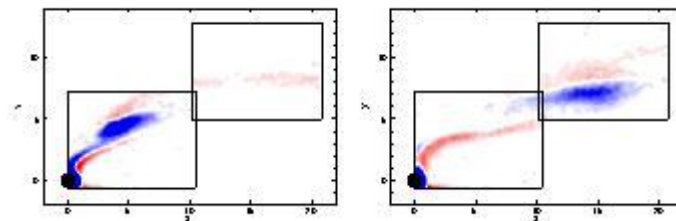


Figure 21 $\alpha = 5.55 -$ vorticity patch

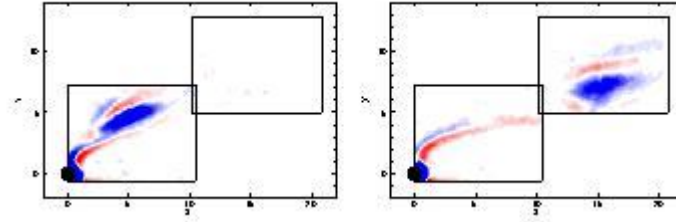


Figure 22 $\alpha = 5.55 - 2$. vortex

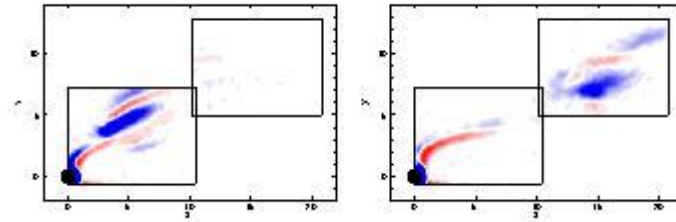


Figure 23 $\alpha = 5.55 - 3$. vortex

(b) Shedding process – $\alpha = 5.55$

The evolution of the second and the third vortices over time are shown in Figures 22 and 23. Their value is at $\alpha = 5.55$ and they are displayed in detail in Figure 24. The coordinates system is non-dimensional with a rotating cylinder in the origin of axis. The blue colour indicates positive vorticity, and the red one negative vorticity. There is not vorticity patch during the evolution of vorticity patterns over time.

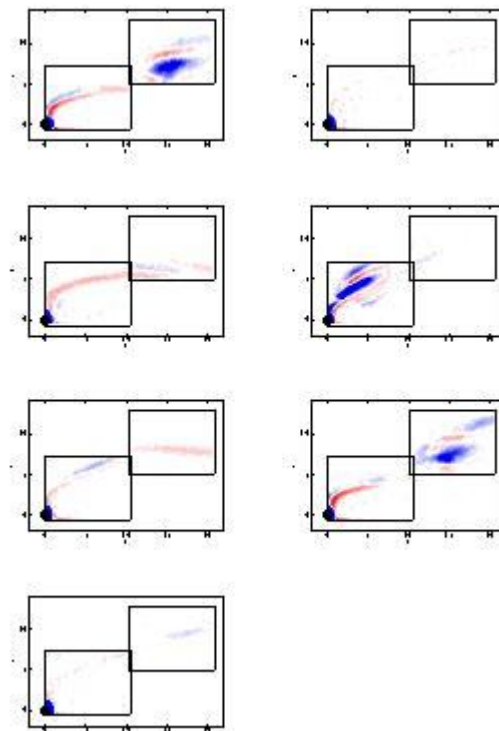


Figure 24 $\alpha = 5.55$ – Shedding process

3.5 Stable region

Further increase of rotational rate of the cylinder results placing the flow again into the stable region. The vortices are suppressed for rotation rate $\alpha > 5.60$, see Figure 25. The coordinate system is non-dimensional. The period T and a Strouhal number can not be calculated without vortices. Therefore, the Strouhal number is $St = 0$.

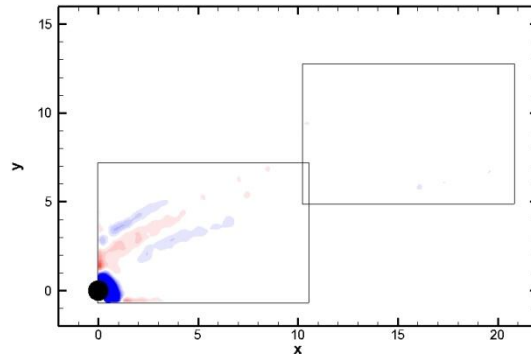
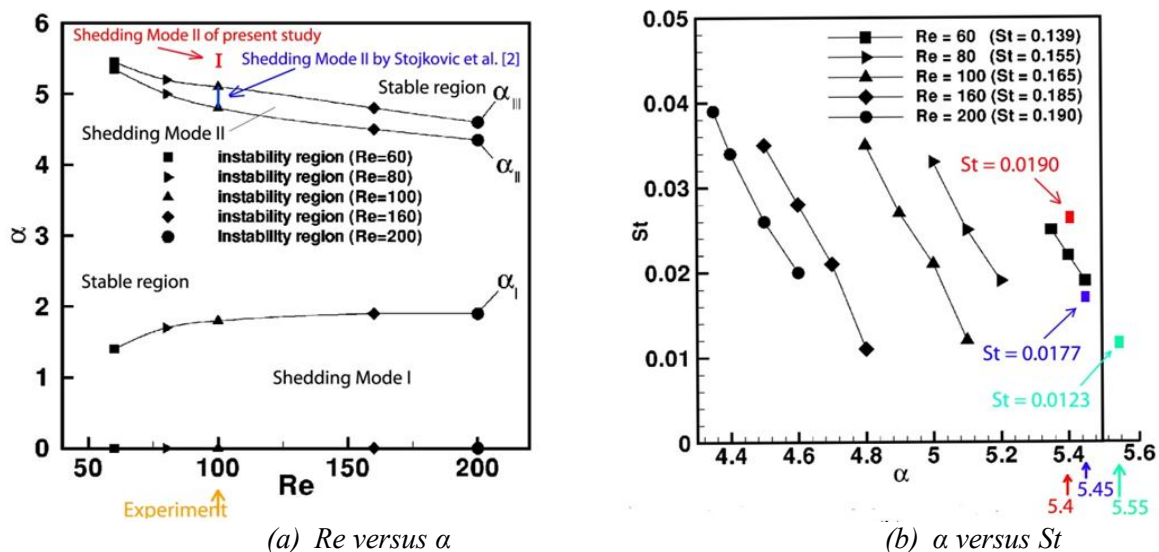


Figure 25 Stable region - $\alpha = 5.60$, $Re = 100$

4. Discussion

The von Karman vortex street, two stable and two unstable regimes were investigated for $Re = 100$. The von Karman vortex street and the first unstable regime – SheddingMode I correspond positively to the previous studies [1–6]. In current experiment it was found out Shedding Mode II of different position in stability diagram. The spaces of the different regions are as such $4.8 \leq \alpha \leq 5.1$ by Stojkovic et al. (2003) [2] or $4.85 \leq \alpha \leq 5.17$ by Pralits et al. (2010) [6].

The results of current experiment are graphically demonstrated in the stability diagram Re versus α , Figure 26 (a). It is observed that the position of the regions in our case has moved upwards in comparison to the results from the previous studies by Stojkovic et al. (2003) [2]. The red colour indicates the present experiment at $5.4 \leq \alpha \leq 5.55$. The blue colour indicates the results by Stojkovic et al. (2003) [2]. Also the Strouhal number has been moved to different positions, as shown in the $\alpha - St$ diagram, Figure 26 (b). The experimentally obtained values are drawn near to low Reynolds numbers.



(a) Re versus α (b) α versus St
 Figure 26 (a) Stability diagram and (b) Diagram for different Re by [2]

The Shedding Mode II investigated by L. Brandt (2008) [8] as a two-dimensional numerical solution with $Re = 100$ at $\alpha = 4.85$ is shown in Figure 27. It is possible to detect that vortex occurs in an approximate position of $x = 16D$ and $y = 4.5D$. The position of the vortex resulted from the current experiment occurs in a position of $x = 16D$ and $y = 6.5D$. That means that the position of the vortex is very similar to the position obtained from the experiment done by L. Brandt.

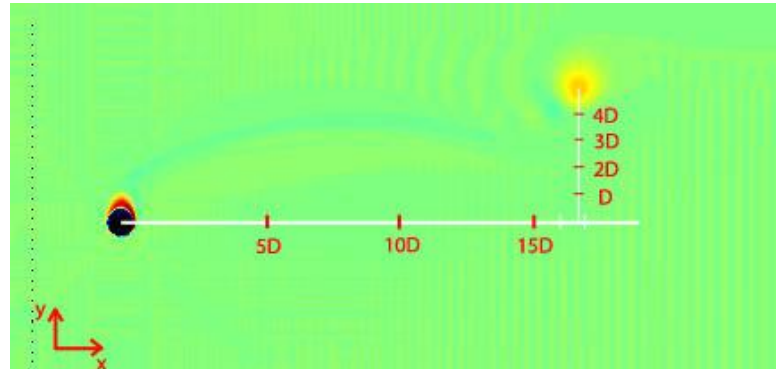


Figure 27 Numerical simulation by L. Brandt – $\alpha = 4.85$, $Re = 100$

The experimental study by Yildirim et al. (2009) [1] for $Re = 100$ at $\alpha = 4.96$ is displayed in Figure 28. These vortices occur in Shedding Mode II. However, their position is very different from L. Brandt (2008) [8] and current study. Four vortices are in the same position as the cylinder and rotates in the counter-clockwise direction, so does the cylinder. The Strouhal number $St \sim 0.017$ is calculated in the experiment by Yildirim et al. (2009) [1] assimilate to the Strouhal number at $\alpha = 5.55$ obtained from this study.

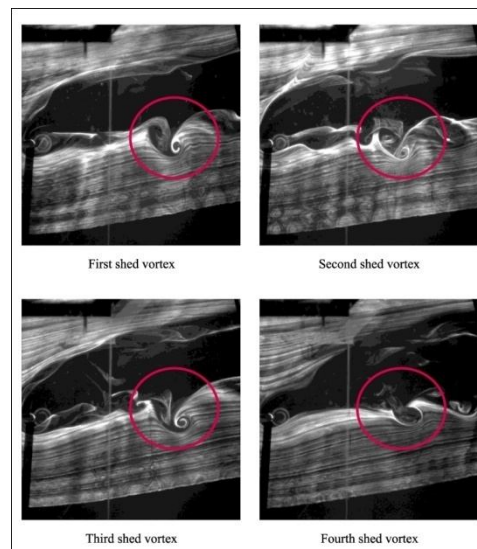


Figure 28 Experimental measurement by Yildirim et al. (2009) [1] - $\alpha = 4.96$, $Re = 100$

5. Conclusion

A flow past a circular cylinder, rotating in the counter-clockwise sense, and subject to in a uniform stream for $Re = 100$ has been analysed for various rotation rates ($0 \leq \alpha \leq 5.6$). The flow is associated with two-dimensional instabilities. The von Karman vortex street, two stable regions and two unstable regions (Shedding Mode I and Shedding Mode II) were found.

The von Karman vortex street is seen in the wake behind the cylinder for $0 \leq \alpha \leq 1.6$ with $St \sim 0.165$ and this regime is called Shedding Mode I. Negative vortex is shed from the upper surface of the cylinder while a positive vortex is released from the lower surface. The vortices are axially symmetrical for a non-rotational case. An increase in the rotational rate is accompanied by an upward deflection of the wake. Therefore, vortex street is deflected away from the centre line for non-zero α and due to the counter-clockwise direction of rotation. The wake becomes narrower and the Strouhal number for vortex shedding decreases with increasing rotational rate. Vortex shedding ceases beyond $\alpha \sim 1.9$ for $Re = 100$.

A steady state at $\alpha = 3.0$ is achieved with increasing α and is found between two unstable regions. The Strouhal number is equal to zero.

The flow loses its stability at $\alpha \sim 5.4$. A second type of instability appears for higher rotational speed at $\alpha = 5.4, 5.45, 5.50, 5.55$. This region is called Shedding Mode II. The vortex shedding appears again but as a single shed vortex in a counter-clockwise sense. The vortex appears only from its upper surface and so on the instability is different than in Shedding Mode I.

Three vortices are usually developed during one measurement except one case at $\alpha = 5.50$ where only vorticity patches occur. The vorticity patch evaluated from vortex shows that rotation is very moderate at that point. The changes of the rotation rate are more noticeable on the upper surface of the cylinder than on the lower surface. The vorticity is dragged with the cylinder in higher rotational rates.

The shedding period amongst the vortices is different so the Strouhal number is calculated as an average value amongst all vortices. The values of calculated Strouhal numbers correspond to the lower Reynolds number in stability diagram. The results of the Strouhal number as well as range of Shedding Mode II match with $Re = 60$ as it can be seen in Figure 26 by Stojkovic et al. (2003) [2]. Further on, the results of experimental measurement for Shedding Mode II are in range $5.4 \leq \alpha \leq 5.55$, while the results from previous studies are in range $4.8 \leq \alpha \leq 5.1$ by Stojkovic et al. (2003) [2] or $4.96 \leq \alpha \leq 5.1$ by Yildirim et al. (2009) [1].

A position of rotating vortices in Shedding Mode II is in agreement with the numerical simulation of L. Brandt (2008) [8], Figure 27. However, the vortices occur on a higher position in comparison with Yildirim et al. (2009) [1], Figure 28.

Vortex shedding continues for higher rotation rates and the flow becomes stable again for $\alpha \geq 5.6$.

Since the flow is not fully developed, the Strouhal number differs for every vortex in each case. It is presumed that if there is sufficient long experimental time. Therefore, either the extension of the towing tank or performing experiments in another channel is required.

Bibliography

- [1] Yildirim, I., Rindt, C.C.M.: *Experimental investigation of Shedding Mode II behind a rotating cylinder*, Energy Technology Division, Department of Mechanical Engineering, Eindhoven University of Technology, Eindhoven, the Netherlands, 2009.
- [2] Stojkovic, D., Schön, P., Breuer, M., Durst, F.: *On the new vortex shedding mode past a rotating circular cylinder*, Physics of Fluids, Vol. 15, No. 5, pp 1257-1260, 2003.
- [3] Kang, S., Choi, H.: *Laminar flow past a rotating circular cylinder*, National CRI Center for Turbulence and Flow Control Research, Institute of Advanced Machinery and Design, Seoul National University, Seoul 151-742, Physics of Fluids, Vol. 11, n. 11, Korea, 1999.
- [4] Mittal, S., Kumar, B.: *Flow past a rotating cylinder*, Journal of Fluid Mechanics, Vol. 476, pp. 303-334, 2003.

- [5] Akoury,R., Braza,M., Perrin, R.,Harran,G.,Hoarau, Y.: *The three-dimensional transition in the flow around a rotating cylinder*, Journal of FluidMechanics, Vol. 607, pp. 1-11, 2008.
- [6] Pralits, J. O., Brandt, L., Giannetti, F.: *Instability and sensitivity of the flow around a rotating circular cylinder*, Cambridge University, J. Fluid Mech., Vol. 650, pp. 513-536, 2010.
- [7] Raffel, M., Willert, C., Wereley, S., Kompenhans, J.: *Particle Image Velocimetry, A Practical Guide*, ISBN 978-3-540-72307-3 Second Edition Springer Berlin Heidelberg New York, 2007.
- [8] Brandt.,L., Personal communication, 2008.
- [9] PivView, Version 1.7, User Manual, <http://www.pivtec.com>